HHS Public Access

Author manuscript

Nature. Author manuscript; available in PMC 2010 April 22.

Published in final edited form as:

Nature. 2009 February 12; 457(7231): 915–919. doi:10.1038/nature07598.

A stress-responsive RNA switch regulates VEGF expression

Partho Sarothi Ray[1,2], **Jie Jia**[1], **Peng Yao**[1], **Mithu Majumder**[3], **Maria Hatzoglou**[3], and **Paul L. Fox**[1,*]

[1]Department of Cell Biology, The Lerner Research Institute, Cleveland Clinic, 9500 Euclid Avenue, Cleveland, Ohio, USA 44195

[2]Department of Biology, Indian Institute of Science Education and Research, Kolkata 700106, India

[3]Department of Nutrition, Case Western Reserve University, 10900 Euclid Avenue, Cleveland, Ohio, USA 44106

Abstract

Ligand binding to structural elements in noncoding regions of mRNA modulates gene expression[1],[2]. Ligands such as free metabolites or other small molecules directly bind and induce conformational changes in regulatory RNA elements known as riboswitches[1]-[4]. Other types of RNA switches are activated by complexed metabolites, e.g., RNA-ligated metabolites such as aminoacyl-charged tRNA in the T-box system[5], or protein-bound metabolites in the glucose- or amino acid-stimulated terminator-antiterminator systems[6],[7]. All of these switch types are found in bacteria, fungi, and plants[8]-[10]. Here, we report an RNA switch in human vascular endothelial growth factor-A (VEGF) mRNA 3'UTR that integrates signals from interferon (IFN)-γ and hypoxia to regulate VEGF translation in myeloid cells. Analogous to riboswitches, the VEGF 3'UTR undergoes a binary conformational change in response to environmental signals. However, the VEGF 3'UTR switch is metabolite-independent, and the conformational change is dictated by mutually exclusive, stimulus-dependent binding of proteins, namely, the IFN-γ-activated inhibitor of translation (GAIT) complex[11],[12] and heterogenous nuclear ribonucleoprotein (hnRNP) L. We speculate the VEGF switch represents the founding member of a family of signal-mediated, protein-dependent RNA switches that evolved to regulate gene expression in multicellular animals where precise integration of disparate inputs may be more important than rapidity of response.

*To whom all correspondence should be addressed: Department of Cell Biology The Lerner Research Institute / NC10 Cleveland Clinic 9500 Euclid Avenue Cleveland, OH 44195 Tel: 216-444-8053; Fax: 216-444-9404; foxp@ccf.org.
E-mail addresses of coauthors: P. S. Ray, psray@iiserkol.ac.in; J. Jia, jiaj@ccf.org; P. Yao, yaop@ccf.org; M. Majumder, mithu.majumder@case.edu; M. Hatzoglou, mxh8@case.edu

Author Information Reprints and permissions information is available at www.nature.com/reprints. Correspondence and requests for materials should be addressed to P.L.F. (foxp@ccf.org).

Full Methods and any associated references are available in the online version of the paper at www.nature.com/nature.

Supplementary Information is linked to the online version of the paper at www.nature.com/nature.

None of the authors have any financial conflict of interest with the information in this manuscript.

VEGF is induced by hypoxic stress in pathological settings such as tumor cores and atherosclerotic lesions[13-15]. These sites are enriched in inflammatory cytokines, including IFN-γ which represses myeloid cell expression of VEGF and other inflammatory proteins by GAIT-mediated translational silencing[16,17]. Macrophages simultaneously exposed to opposing inflammatory and hypoxic signals must render a decision to restrict GAIT function to allow VEGF synthesis and risk inflammatory protein accumulation, or permit GAIT-mediated inhibition of VEGF synthesis and risk unrelieved hypoxia. To determine the cell response to this dilemma, U937 monocytic cells were exposed simultaneously to hypoxia and IFN-γ. The decrease in VEGF protein after normoxic, IFN-γ treatment for 24 h was completely abrogated by hypoxia (Fig. 1a, Suppl. Fig. 1). Polysome profiling and RT-PCR (or qRT-PCR) showed that hypoxia restored VEGF translation (Suppl. Figs. 2,3). Consistent with other reports, mild hypoxia inhibited total protein synthesis nominally (Suppl. Fig. 4)[18]. Thus, hypoxia overrides GAIT-mediated repression of VEGF translation observed in normoxia[16].

To determine whether hypoxia inhibits the GAIT pathway or specifically alters VEGF mRNA response to IFN-γ, we compared *in vitro* translation of firefly luciferase (Fluc) reporter transcripts bearing ceruloplasmin (Cp) and VEGF mRNA 3'UTRs, both containing functional GAIT elements[16,19]. Lysates from normoxic, but not hypoxic, cells treated with IFN-γ for 24 h repressed translation of the VEGF 3'UTR-bearing reporter (Fig. 1b). In contrast, both lysates blocked translation of Cp 3'UTR-bearing reporter, indicating a functional GAIT complex in hypoxia. RNA EMSA/supershift analysis verified binding-competent GAIT complex in hypoxic lysates (Suppl. Fig. 5). Thus, a hypoxic cells factor(s) specifically overcomes silencing of VEGF mRNA translation, implicating a VEGF 3'UTR-related property.

The VEGF 3'UTR contains a 125-nt, hypoxia stability region (HSR) that binds hnRNP L, a splicing factor with cytosolic activities[20] including mRNA stabilization[21,22] (Fig. 1c). The VEGF GAIT element resides within the HSR, immediately downstream of the hnRNP L binding site. Translation of a reporter transcript bearing the HSR was inhibited by 24-h, IFN-γ-treated normoxic, but not hypoxic, lysate (Fig. 1d). In contrast, translation of a transcript bearing VEGF GAIT element alone was silenced by both lysates. Expression of HSR-bearing reporter in U937 cells treated with IFN-γ was also restored under hypoxia, whereas a reporter containing only the GAIT element was repressed under both normoxia and hypoxia (Fig. 1e). Thus, the HSR recapitulates the differential response of VEGF mRNA to IFN-γ and hypoxia *in vitro* and *in vivo*. Similar results were observed in primary human peripheral blood monocytes, murine bone marrow-derived macrophages, and other human and murine myeloid cell lines (Suppl. Fig. 6). Glutamyl-prolyl tRNA synthetase (EPRS) is the GAIT protein that binds GAIT element RNA[12,23]. UV-crosslinking of the HSR with lysates from IFN-γ-treated cells revealed an ~170 kDa protein consistent with EPRS that binds only under normoxia (Fig. 2a). The interaction of a ~60 kDa protein consistent with hnRNP L was enhanced by hypoxia[22]. These bands were identified as hnRNP L (Fig. 2a, left) and EPRS (Fig. 2a, right) by immunodepletion. Notably, depletion of hnRNP L induces EPRS binding to the HSR, even in hypoxia, and the converse was seen after EPRS depletion, suggesting mutually exclusive binding of hnRNP L and EPRS.

$AS_{3'UTR,332-357}$, an oligomer antisense to the reported hnRNP L binding site[22], markedly decreased hnRNP L binding to HSR RNA in hypoxic cell lysates (Fig. 2b) and restored translation inhibition of an HSR-bearing reporter RNA in the presence of 24-h, IFN-γ-treated, hypoxic cell lysates, indicating hnRNP L binding is required to overcome translation silencing (Fig. 2c). Likewise, exogenous expression of myc-tagged hnRNP L in IFN-γ-treated, normoxic cells partially restored expression of VEGF (Suppl. Fig. 7a) and VEGF HSR-containing reporter (Suppl. Fig. 7b). Mutation of the HSR CA-repeats abrogated binding of recombinant hnRNP L (Suppl. Fig. 8a) and overcame translation repression by normoxic IFN-γ treatment (Suppl. Fig. 8b). Similarly, U-to-C mutation in HSR nt position 367 (which is essential for GAIT complex binding[16]) blocked binding of recombinant EPRS linker (the domain that binds the GAIT element[23]), and repressed translation even under hypoxia. Lastly, siRNA-mediated knockdown confirmed the requirement for hnRNP L in regulating expression of endogenous VEGF (Fig. 2d) and VEGF HSR-bearing reporter (Suppl. Fig. 9). VEGF expression was not repressed by IFN-γ treatment of normoxic cells in which GAIT complex formation is prevented by knockdown of the essential GAIT component, ribosomal protein L13a (Suppl. Fig 10)[11].

Surface plasmon resonance showed hnRNP L (K_d = 61.5 nM) and EPRS linker (K_d = 26.4 nM) have comparable affinity for VEGF HSR RNA, suggesting they might compete for binding, and the equilibrium could be shifted by changes in their relative amounts. Hypoxia did not increase hnRNP L expression (Fig. 3a). However, IFN-γ treatment in normoxia markedly reduced hnRNP L expression, and hypoxia partially blocked this decrease. MG132, a proteasome inhibitor, blocked IFN-γ-mediated reduction of hnRNP L (Fig. 3b). Also, MG132 overcame translational silencing *in vitro* (Fig. 3c) and in transfected cells (Suppl. Fig. 11). Thus, hypoxia overcomes the IFN-γ-stimulated proteasomal degradation of hnRNP L and maintains a level of hnRNP L protein that competes with the GAIT complex for HSR binding.

The proximity of hnRNP L and GAIT complex binding sites suggests a potential interaction contributing to mutually exclusive binding. The lowest energy (−17.3 kcal/mol) predicted secondary structure[24] of the HSR is stabilized by a 25-bp stem (Fig. 4a, left). The experimentally defined GAIT structural element[19] is disrupted by base-pairing with a downstream antisense strand (stem stability sequence). The lack of a GAIT element structure suggests this predicted conformer is “translation-permissive” (TP). Because GAIT complex binding to the HSR under normoxia requires GAIT element recognition, we re-folded the HSR under experimentally determined base-pairing constraints essential for GAIT element structure and function[19], which predicted a “translation-silencing” (TS) conformer less stable (−4.1 kcal/mol) than the TP conformer (Fig. 4a, right). We hypothesized that VEGF HSR RNA might exist in both conformations, and that hypoxia and IFN-γ regulate a binary switch between the conformations mediated by mutually exclusive binding of hnRNP L and GAIT complex.

To validate the RNA switch experimentally, *in vitro*-transcribed HSR was subjected to RNase A probing[25]. Nearly all nuclease cleavage sites corresponded to nucleotides predicted to be single-stranded in both conformers (Fig. 4a; 4b, lane 2). A notable exception was cleavage at UTR positions 359 and 361 (GE1), predicted to be a single-stranded bulge in the

TP, but base-paired in the TS conformer. Cleavage at positions 371 and 374 (GE2) exhibited opposite characteristics, i.e., base-paired in the TP but single-stranded in the TS conformer. Robust cleavage at GE1 and GE2 suggested co-existence of both conformers. The presence of the less energetically favorable TS conformer can be explained by co-transcriptional folding, i.e., sequential folding of subdomains in nascent mRNA during transcription[26]. Heat-denaturation and subsequent renaturation of the HSR eliminated the GE2 signature, establishing the presence of two conformers and a conformational switch (Fig. 4c, lanes 1,2). Finally, we investigated the role of proteins in the RNA switch. The HSR was incubated with lysates from IFN-γ-treated cells, protein was removed, and extracted RNA probed with RNase A[27]. Normoxic cell lysate decreased GE1 cleavage, consistent with conversion to the TS conformer (Fig. 4d, lane 2). Conversely, hypoxic lysate induced conversion to the TP conformer (lane 5). In normoxic lysates, immunodepletion of GAIT complex switched most RNA to the TP conformer (lane 3), whereas hnRNP L depletion caused conversion to the TS conformer (lane 4). In hypoxic lysates, hnRNP L depletion partially restored the TS conformer (lane 7). These data reveal a protein-dependent, hypoxia- and IFN-γ-responsive RNA switch in the VEGF 3'UTR that regulates translation.

The VEGF RNA switch is functionally analogous to bacterial riboswitches, undergoing conformational changes in response to environmental signals to regulate gene expression. However, the sensing mechanisms of the switches are distinct. Riboswitches respond to stimuli by direct binding of the effector molecule. In contrast, the VEGF switch requires signal "interpretation" by regulatory proteins (Fig. 4e). VEGF mRNA uses an unprecedented switching mechanism to integrate the response to two disparate stress stimuli. The switch comprises a single domain that alternates between two conformers in response to mutually exclusive binding of ligands, thereby functioning as an uncommon "AND NOT" Boolean logic gate (Fig. 4f) distinct from the S-adenosyl methionine and adenosylcobalamin riboswitches in *B. clausii* metE mRNA which bind their cognate ligands independently to form a NOR logic gate[28]. Multi-input signal integration may be advantageous for regulating gene expression in response to the diverse environmental stresses faced by metazoan cells. The switch may be myeloid cell-specific, as EPRS binding and VEGF translational repression are not seen in HeLa cells (Suppl. Fig. 12). Transcript specificity permits GAIT-mediated repression of harmful inflammatory proteins while simultaneously allowing high-level VEGF expression to relieve tissue hypoxia[15]. We anticipate that elements in other eukaryotic transcripts will be discovered as components of RNA switches. A small upstream ORF in arginine transporter cat-1 mRNA internal ribosome entry site is a candidate as it undergoes a conformational change in response to amino acid availability; however, regulatory proteins have not been identified[29]. The VEGF switch may represent the founding member of a family of protein-dependent binary RNA switches in which environmental stimuli are transduced by regulatory proteins to alter RNA conformation and control gene expression.

METHODS SUMMARY

Human U937 monocytic cells were incubated with 500 units/ml of human IFN-γ (R & D Systems) for up to 24 h. Hypoxic treatment was in a humidified incubator at 3% pO_2. Capped RNAs were transcribed from linearized plasmids using the mMessage mMachine

transcription system (Ambion). [α-^{32}P]UTP-labeled VEGF-HSR RNA was transcribed using the T7-riboprobe system (Promega). RNAs were *in vitro* translated in rabbit reticulocyte lysate (Promega) in the presence of methionine-free amino acid mixture and translation-grade [^{35}S]methionine (Perkin Elmer) and cytosolic extract (500 ng of protein). Cells were nucleofected (Amaxa) with siRNAs or reporter plasmids containing Fluc upstream of wild-type or mutant VEGF HSR expressed from CMV promoter, together with Rluc driven by SV40 promoter. For analysis of polysome-associated mRNA, ribosomal fractions were obtained by sucrose gradient fractionation[30]. RNA was isolated using Trizol reagent (Life Technologies) and subjected to RT using oligo(dT) primers and PCR using gene-specific primers. The conformational switch in the VEGF HSR RNA was probed by enzymatic cleavage by RNase A (Ambion). To probe protein-dependent RNA conformational shifts, proteins were removed with 5% SDS on ice before RNA extraction with phenol:chloroform and precipitation by ethanol in presence of 2 mM $MgCl_2$[27].

METHODS

Plasmid construction

The pSP64-FLuc-VEGF-A 3'UTR$_{(11\text{-}900)}$-A$_{30}$, pSP64 FLuc-Cp 3'UTR-A$_{30}$, and pSP64-FLuc-VEGF-A GAIT-A$_{30}$ constructs were generated as described[15],[31]. The VEGF-A 3'UTR HSR sequence (nt 332-456) was PCR-amplified and inserted into the pcDNA3 vector (Invitrogen) to generate pcDNA3-VEGF-A HSR. The VEGF-A HSR sequence was also inserted into pSP64-FLuc-VEGF-A 3'UTR$_{(11\text{-}900)}$-A$_{30}$ after releasing the VEGF-A 3'UTR to generate pSP64-FLuc-VEGF-A HSR-A$_{30}$. The VEGF HSR was also inserted downstream of FLuc in pcDNA3 to generate pCD-FLuc-VEGF-A HSR. VEGF-A HSR, with U367 mutated to C, was PCR-amplified by a megaprimer approach and the mutated sequence was also inserted downstream of FLuc in pcDNA3 to generate pCD-FLuc-VEGF-A HSR-GAITmut. The VEGF-A HSR was also amplified using a forward primer with the C and A residues in the hnRNP L binding site mutated to G and T respectively, to generate VEGF-A HSR-hnRNP L sitemut. The sequence was inserted downstream of FLuc in pcDNA3 to generate pCD-FLuc-VEGF-A HSR-hnRNP L site-mut. Both the mutant sequences were also inserted into pcDNA3 to generate the template for in vitro transcription. The pcDNA3-myc-hnRNP L plasmid was a kind gift from Naoyuki Kataoka, University of Pennsylvania School of Medicine. Rat hnRNP L sequence was inserted into a His-tagged prokaryotic expression vector for bacterial expression. The linker domain of human EPRS (aa 753-953) was similarly expressed from a His-tagged prokaryotic expression vector.

Immunodepletion of GAIT Complex and hnRNP L

U937 cell lysates were incubated with polyclonal anti-EPRS antibody[15] or polyclonal anti-hnRNP L antibody (Santa Cruz) coupled to protein-A Sepharose CL beads (Sigma) in RIPA buffer. The beads were pelleted and the process was repeated twice with supernatants. The supernatants were concentrated and re-dissolved in 10X PBS. The supernatants were immunoblotted with anti-EPRS and anti-hnRNP L antibody to verify immunodepletion.

Isolation of Polysome-Associated mRNA

Ribosomal fractions were obtained as described[30]. Briefly, U937 cells were homogenized in TMK lysis buffer containing cycloheximide (0.1 mg/ml). Cells were lysed and cytosolic extract was obtained by centrifugation at 10,000 × g for 20 min. The extract was overlayed on a 10-50% (w/v) sucrose gradient and centrifuged at 100,000 × g for 4 h at 4 °C. Fractions were collected using a programmable gradient fractionator (Isco) and absorbance at 254 nm was measured.

Cell Transfection and Luciferase assay

U937 cells were transiently co-transfected with 6 μg of pCD-FLuc-VEGF-A HSR and 8 μg of pCD-myc-hnRNPL DNAs using human dendritic cell nucleofection kit V (Amaxa Biosystems). RLuc-expressing vector pRL-SV40 (1 μg) was co-transfected for normalization of transfection efficiency. After 12 h, transfected cells were incubated with IFN-γ, lysed, and either immunoblotted or luciferase activity of the lysate was measured using dual luciferase assay kit (Promega). Cells were similarly nucleofected with 400 nM siRNA against hnRNP L (target sequence: 1066-1084, UAUGGCUUGGAUCAAUCUA) or with a control siRNA which is not similar to any human genomic sequence (AAGCGCTACT-ACAGCAGTC).

UV-crosslinking of RNA-protein complexes

^{32}P-UTP labeled RNAs were incubated with cell lysates or bacterially-expressed and purified EPRS linker or rat hnRNP L proteins and then UV-crosslinked. The RNA-protein complexes were extensively digested by RNase A digestion and resolved by SDS-PAGE

Computational prediction of RNA structure

RNA secondary structure predictions of the VEGF HSR RNA were performed using the Mfold program (http://mfold.bioinfo.rpi.edu), and the structure with the lowest free energy selected. The same sequence was refolded by incorporating base-pairing constraints in the GAIT element stems that have been experimentally determined to be required for GAIT complex binding and activity[18].

Enzymatic probing of RNA Structure

VEGF-A HSR RNA was generated by *in vitro* transcription, and then 5′-end-labeled with [γ-^{32}P]ATP using the KinaseMax kit (Ambion). The RNA was purified using Micro Bio-Spin chromatography columns (Biorad) and the purity tested on 8 M urea-5% polyacrylamide gel. The RNA was probed with RNase A (Ambion) as described[24] with modifications. Briefly, about 10,000 cpm of the end-labeled RNA, together with 3 μg of yeast tRNA, was incubated with 10 pg of RNase A in 1X RNA structure buffer for 10 min at room temperature. Amounts of RNase used in the reactions were initially titrated to ensure “single-hit” cleavage. For RNA sequencing reactions, similar amounts of end-labeled RNA and tRNA was incubated with 20 pg of RNase A in 1X sequencing buffer at 50 °C for 5 min. The single nucleotide ladder was generated by incubating similar amounts of end-labeled RNA and tRNA in hydroxide hydrolysis buffer (50 mM NaOH, 1 mM EDTA) at 90

°C for 3 min. The reactions were resolved on 8 M urea-10% polyacrylamide sequencing gels.

For probing the protein-directed RNA conformational change, extraction of end-labeled RNA after protein-binding was done as described previously[26] with modifications. Briefly, the RNA was incubated with 100 ng of cell lysates, and immundepleted lysates, in RNA binding buffer at room temperature for 15 min. Proteins were removed by incubation with 2 μl of 5% SDS on ice. The RNA was extracted twice with phenol:chloroform and precipitated by ethanol in presence of 2 mM $MgCl_2$. The RNA was further subjected to RNase digestion as described above.

Supplementary Material

Refer to Web version on PubMed Central for supplementary material.

Acknowledgements

We are grateful to D. Driscoll and T.M. Henkin for helpful discussions. This work was supported by NIH grants P01 HL29582, R01 HL67725, and P01 HL76491 (to P.L.F.), and R01 DK60596 (to M.H.).

REFERENCES

1. Mandal M, Breaker RR. Gene regulation by riboswitches. Nat Rev Mol Cell Biol. 2004; 5:451–463. [PubMed: 15173824]
2. Grundy FJ, Henkin TM. Regulation of gene expression by effectors that bind to RNA. Curr Opin Microbiol. 2004; 7:126–131. [PubMed: 15063848]
3. Winkler W, Nahvi A, Breaker RR. Thiamine derivatives bind messenger RNAs directly to regulate bacterial gene expression. Nature. 2002; 419:952–956. [PubMed: 12410317]
4. Cromie MJ, Shi Y, Latifi T, Groisman EA. An RNA sensor for intracellular Mg^{2+} Cell. 2006; 125:71–84. [PubMed: 16615891]
5. Grundy FJ, Henkin TM. tRNA as a positive regulator of transcription antitermination in B. subtilis. Cell. 1993; 74:475–482. [PubMed: 8348614]
6. Merino E, Babitzke P, Yanofsky C. trp RNA-binding attenuation protein (TRAP)-trp leader RNA interactions mediate translational as well as transcriptional regulation of the Bacillus subtilis trp operon. J Bacteriol. 1995; 177:6362–6370. [PubMed: 7592410]
7. Schilling O, Langbein I, Muller M, Schmalisch MH, Stulke J. A protein-dependent riboswitch controlling ptsGHI operon expression in Bacillus subtilis: RNA structure rather than sequence provides interaction specificity. Nucleic Acids Res. 2004; 32:2853–2864. [PubMed: 15155854]
8. Batey RT. Structures of regulatory elements in mRNAs. Curr Opin Struct Biol. 2006; 16:299–306. [PubMed: 16707260]
9. Cheah MT, Wachter A, Sudarsan N, Breaker RR. Control of alternative RNA splicing and gene expression by eukaryotic riboswitches. Nature. 2007; 447:497–500. [PubMed: 17468745]
10. Wachter A, Tunc-Ozdemir M, Grove BC, Green PJ, Shintani DK, Breaker RR. Riboswitch control of gene expression in plants by splicing and alternative 3′ end processing of mRNAs. Plant Cell. 2007; 19:3437–3450. [PubMed: 17993623]
11. Mazumder B, Sampath P, Seshadri V, Maitra RK, DiCorleto P, Fox PL. Regulated release of L13a from the 60S ribosomal subunit as a mechanism of transcript-specific translational control. Cell. 2003; 115:187–198. [PubMed: 14567916]
12. Sampath P, Mazumder B, Seshadri V, Gerber CA, Chavatte L, Kinter M, Ting SM, Dignam JD, Kim S, Driscoll DM, Fox PL. Noncanonical function of glutamyl-prolyl-tRNA synthetase: gene-specific silencing of translation. Cell. 2004; 119:195–208. [PubMed: 15479637]

13. Braunstein S, Karpisheva K, Pola C, Goldberg J, Hochman T, Yee H, Cangiarella J, Arju R, Formenti SC, Schneider RJ. A hypoxia-controlled cap-dependent to cap-independent translation switch in breast cancer. Mol Cell. 2007; 28:501–512. [PubMed: 17996713]
14. Bastide A, Karaa Z, Bornes S, Hieblot C, Lacazette E, Prats H, Touriol C. An upstream open reading frame within an IRES controls expression of a specific VEGF-A isoform. Nucleic Acids Res. 2008; 36:2434–2445. [PubMed: 18304943]
15. Ferrara N, Davis-Smyth T. The biology of vascular endothelial growth factor. Endocr Rev. 1997; 18:4–25. [PubMed: 9034784]
16. Ray PS, Fox PL. A post-transcriptional pathway represses monocyte VEGF-A expression and angiogenic activity. EMBO J. 2007; 26:3360–3372. [PubMed: 17611605]
17. Mukhopadhyay R, Ray PS, Arif A, Brady AK, Kinter M, Fox PL. DAPK-ZIPK-L13a axis constitutes a negative-feedback module regulating inflammatory gene expression. Mol Cell. 2008 In press.
18. Liu L, Cash TP, Jones RG, Keith B, Thompson CB, Simon MC. Hypoxia-induced energy stress regulates mRNA translation and cell growth. Mol Cell. 2006; 21:521–531. [PubMed: 16483933]
19. Sampath P, Mazumder B, Seshadri V, Fox PL. Transcript-selective translational silencing by gamma interferon is directed by a novel structural element in the ceruloplasmin mRNA 3′ untranslated region. Mol Cell Biol. 2003; 23:1509–1519. [PubMed: 12588972]
20. Piñol-Roma S, Swanson MS, Gall JG, Dreyfuss G. A novel heterogeneous nuclear RNP protein with a unique distribution on nascent transcripts. J Cell Biol. 1989; 109:2575–2587. [PubMed: 2687284]
21. Claffey KP, Shih SC, Mullen A, Dziennis S, Cusick JL, Abrams KR, Lee SW, Detmar M. Identification of a human VPF/VEGF 3′ untranslated region mediating hypoxia-induced mRNA stability. Mol Biol Cell. 1998; 9:469–481. [PubMed: 9450968]
22. Shih SC, Claffey KP. Regulation of human vascular endothelial growth factor mRNA stability in hypoxia by heterogeneous nuclear ribonucleoprotein L. J Biol Chem. 1999; 274:1359–1365. [PubMed: 9880507]
23. Jia J, Arif A, Ray PS, Fox PL. WHEP domains direct noncanonical function of glutamyl-prolyl tRNA synthetase in translational control of gene expression. Mol Cell. 2008; 29:679–690. [PubMed: 18374644]
24. Jaeger JA, Turner DH, Zuker M. Improved predictions of secondary structures for RNA. Proc Natl Acad Sci U S A. 1989; 86:7706–7710. [PubMed: 2479010]
25. Knapp G. Enzymatic approaches to probing RNA secondary and tertiary structure. Methods Enzymol. 1989; 180:192–212. [PubMed: 2482414]
26. Brion P, Westhof E. Hierarchy and dynamics of RNA folding. Annu Rev Biophys Biomol Struct. 1997; 26:113–137. [PubMed: 9241415]
27. Huthoff H, Berkhout B. Two alternating structures of the HIV-1 leader RNA. RNA. 2001; 7:143–157. [PubMed: 11214176]
28. Sudarsan N, Hammond MC, Block KF, Welz R, Barrick JE, Roth A, Breaker RR. Tandem riboswitch architectures exhibit complex gene control functions. Science. 2006; 314:300–304. [PubMed: 17038623]
29. Yaman I, Fernandez J, Liu H, Caprara M, Komar AA, Koromilas AE, Zhou L, Snider MD, Scheuner D, Kaufman RJ, Hatzoglou M. The zipper model of translational control: a small upstream ORF is the switch that controls structural remodeling of an mRNA leader. Cell. 2003; 113:519–531. [PubMed: 12757712]
30. Merrick WC, Hensold JO. Analysis of eukaryotic translation in purified and semipurified systems. Curr Protocols Cell Biol. 2001 Chapter 11.
31. Mazumder B, Seshadri V, Imataka H, Sonenberg N, Fox PL. Translational silencing of ceruloplasmin requires the essential elements of mRNA circularization: Poly(A) tail, poly(A)-binding protein, and eukaryotic translation initiation factor 4G. Mol Cell Biol. 2001; 21:6440–6449. [PubMed: 11533233]

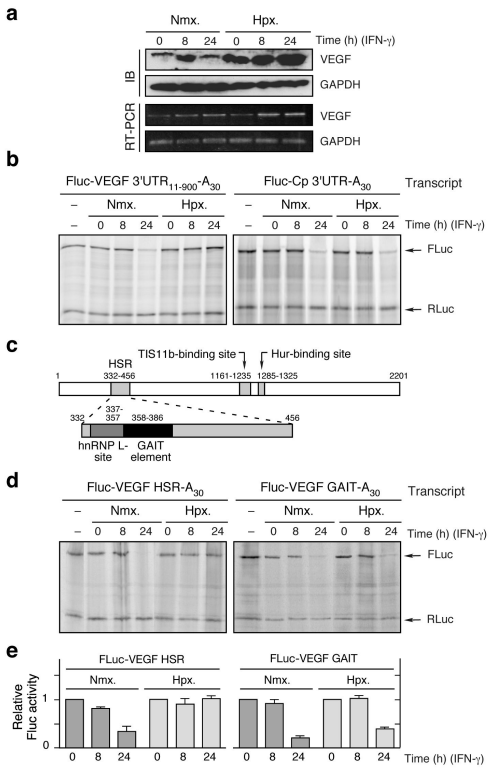

Figure 1. Suppression of GAIT-mediated translation silencing of VEGF by hypoxia

a, VEGF in lysates from U937 cells treated with IFN-γ in normoxia (Nmx.) or hypoxia (Hpx.) was determined by immunoblot (IB) and RT-PCR; GAPDH was probed as control. **b**, *In vitro* translation of Fluc reporter RNAs bearing VEGF 3'UTR$_{11\text{-}900}$ (left) or Cp 3'UTR (right) in presence of cytosolic lysates and control Rluc RNA lacking a 3'UTR. **c**, Schematic of RNA elements in VEGF 3'UTR and HSR. **d**, *In vitro* translation of reporter RNAs bearing VEGF HSR (left) or GAIT element (right) in presence of cytosolic lysates. **e**, U937 cells were nucleofected with pcDNA3-Fluc reporters bearing VEGF HSR (top) or GAIT element (bottom). Cells were co-transfected with a plasmid expressing Rluc under SV40 promoter. Relative luciferase activity (Fluc/Rluc) was expressed as mean ± s.d. (3 experiments).

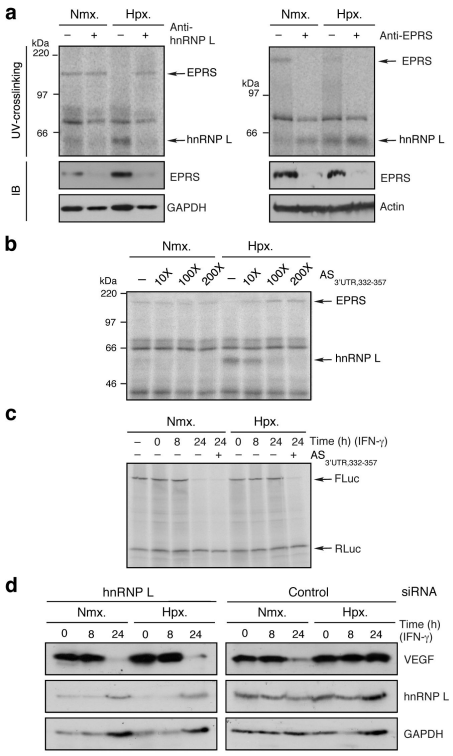

Figure 2. hnRNP L binding to HSR restores VEGF translation in hypoxia

a, Lysates from IFN-γ-treated cells were subjected to UV-crosslinking with [^{32}P]UTP-labeled VEGF HSR RNA before and after immunodepletion with anti-hnRNP L (left) or anti-EPRS (right) antibodies. Effective depletion was shown by IB. **b**, Excess DNA oligomer antisense to hnRNP L binding site ($AS_{3'UTR,332-357}$) blocks binding of hnRNP L to HSR RNA. **c**, Inhibition of hnRNP L binding by $AS_{3'UTR,332-357}$ restores translational silencing of reporter RNA in hypoxia. **d**, siRNA-mediated knockdown of hnRNP L induces translational repression of VEGF in hypoxic cells. Lysates from cells transfected with hnRNP L (left) and control (right) siRNAs were immunoblotted with anti-VEGF, -hnRNP L and -GAPDH antibodies.

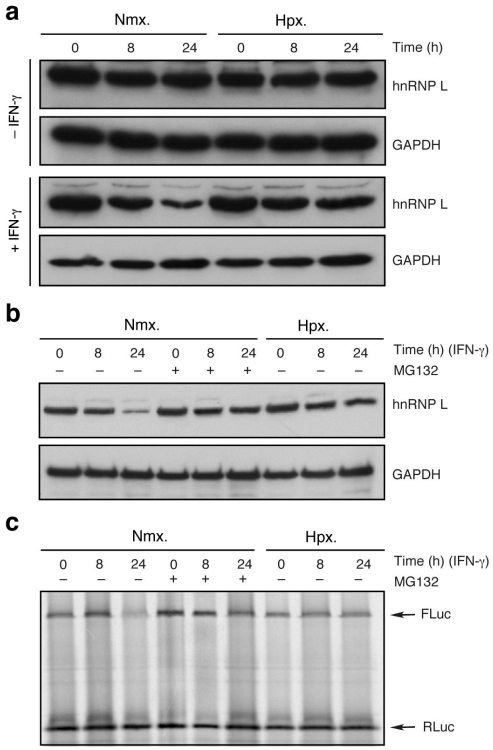

Figure 3. hnRNP L is regulated by stimulus-dependent proteasomal degradation

a, Lysates from U937 cells incubated in the absence or presence of IFN-γ were immunoblotted with anti-hnRNP L and -GAPDH antibodies. **b**, Immunoblot of lysates from cells treated with MG132 (200 nM). **c**, *In vitro* translation of VEGF HSR reporter RNA in presence of cell lysates.

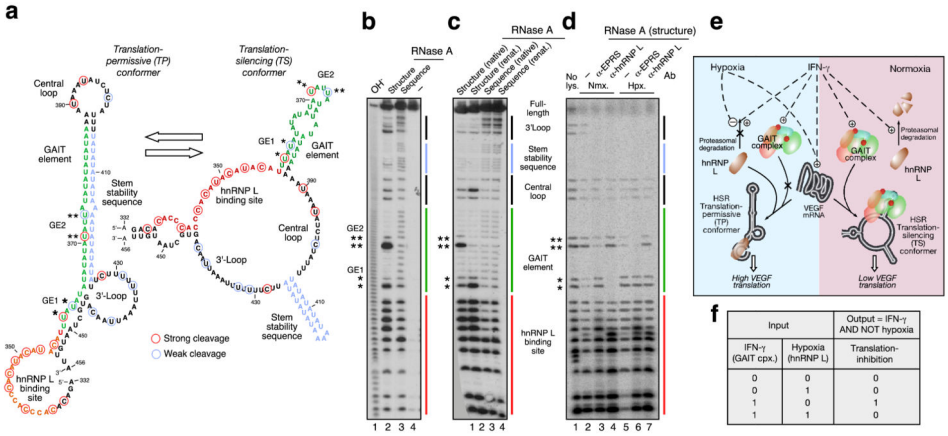

Figure 4. Protein-dependent switching of the VEGF 3'UTR HSR

a, Secondary structure of VEGF HSR predicted by Mfold shows GAIT element (green), hnRNP L binding site (red), and stem stability sequence (blue). TP is lowest free energy conformer predicted by Mfold (left). TS conformer was generated by introducing experimentally-determined base-pairing constraints in GAIT element stem (right). Strong and weak RNase cleavage sites are marked by red and blue circles, respectively. Key signature cleavage sites are indicated (*, **). **b**, ^{32}P-endlabeled VEGF HSR RNA was probed with RNase A under non-denaturing (lane 2) and denaturing (lane 3) conditions. Cleavages corresponding to predicted signature sites are indicated (*, **). **c**, RNase A probing of VEGF HSR RNA under non-denaturing conditions, or after the RNA was denatured and renatured. **d**, VEGF HSR RNA was incubated with cell lysates treated with IFN-γ for 24 h under normoxia or hypoxia, or with lysates immunodepleted with anti-hnRNP L and anti-EPRS antibodies, and subjected to RNase A-mediated cleavage under non-denaturing conditions after protein removal. **e**, Proposed pathway that switches the VEGF HSR to the TP conformer in the presence of IFN-γ and hypoxia (left), or to the TS conformer in the presence of IFN-γ and normoxia (right). **f**, Truth table showing AND NOT Boolean logic function of the VEGF RNA switch integrating signals from IFN-γ and hypoxia.